Fibrinolytic activity of matrix metalloprotease-1

Lokender Kumar[1,#], Joan Planas-Iglesias[2,3#], Chase Harms[1], Sumaer Kamboj[1], Judith Klein-Seetharaman[2,4,*], and Susanta K. Sarkar [1, *]

[1]*Department of Physics, Colorado School of Mines, 1500 Illinois Street, CO 80401, USA*
[2]*Warwick Medical School, University of Warwick, Coventry CV4 7AL, UK*
[3]*Loschmidt Laboratories, Department of Experimental Biology, Faculty of Science, Masaryk University, Kamenice 5/A13, 625 00 Brno, Czech Republic*
[4]*Department of Chemistry, Colorado School of Mines, 1500 Illinois Street, CO 80401, USA*

[#]*These authors contributed equally*

Corresponding author:
[*]ssarkar@mines.edu

ABSTRACT

While the roles of protein conformational dynamics and allostery in protein function are well-accepted concepts, the roles of inter-domain dynamics in the structure-dynamics-function relation of biomolecules are not yet completely understood. Here we show that inter-domain dynamics of matrix metalloprotease-1 (MMP1) on fibrin are correlated with activity and can be modulated using ligands. Using single-molecule Forster Resonance Energy Transfer (FRET), we determined that the distance between the catalytic and hemopexin domains of MMP1 becomes larger/smaller as the MMP1 activity becomes higher/lower. We modulated the activity using 1) a point mutation E219Q at the catalytic site of MMP1, which renders MMP1 inactive on its well-known substrate collagen and 2) tetracycline, an inhibitor of MMP1. At the ensemble level, MMP1 degraded the three chains of fibrin in a specific order with the α-chain first and the γ-chain last. The experimentally observed sequence of degradation can be explained by calculating the distance between atoms of MMP1 and the three chains from the molecular docking poses, which showed that the proximity of MMP1 to the α-chain had the lowest average value and the γ-chain has the largest average value. MMP1 degraded and dissolved crosslinked fibrin efficiently within hours. Our results pave a way towards the molecular understanding of MMP1 promiscuity by correlating inter-domain allosteric communications with activity.

Keywords: Inter-domain dynamics and activity, MMP1 conformational dynamics on fibrin, Single-molecule FRET.

Matrix metalloproteases (MMPs) are broad-spectrum proteases that are capable of degrading many matrix and non-matrix proteins[1]. MMPs are particularly known for their ability to degrade collagen, the primary components of the extracellular matrix (ECM) that provide a scaffold for cells to maintain tissue integrity[2]. MMPs are calcium- and zinc-dependent enzymes with 23 members in the family that are produced by cells in pro forms, i.e., they need to be activated by cleaving off the pro domain for activity[2,3]. MMP1, a collagenase that degrades triple-helical type-1 collagen, stands out in the 23-member MMP family because it has crystal structure available[4] and its interaction with collagen monomers is well-studied[5-13]. MMP1 consists of a catalytic domain that actually degrades substrates, a hemopexin domain that helps MMPs bind to the substrates, and a linker that mediates communications between the two domains (**Figure 1**). MMPs are highly promiscuous, an attribute that we previously used to degrade *E. coli* proteins and purified recombinant MMP1 using a protease-based method[14]. The promiscuity of MMPs is intriguing because the catalytic domain sequence is largely conserved across the MMP family, whereas the hemopexin domain sequence varies[15,16]. Indeed, the hemopexin domain has been shown to influence substrate/ligand specificity and activation/inhibition of various MMPs[17] and regulation of MMP1 catalytic activity by the hemopexin domain has been reported[6]. These results suggest that differences in activity and substrate specificity among MMPs are likely caused by allosteric (far from the catalytic site) communications from other domains. Recently, we showed that inter-domain dynamics of MMP1 on collagen fibrils correlate with activity and the two domains can allosterically communicate via the linker region as well as the substrate.

In this paper, we focus on MMP1 inter-domain dynamics on fibrin, the primary component of a blood clot. Fibrin is an important physiological substrate because ~900000 patients are diagnosed with complications from clot formation leading to ~300,000 deaths[18] and ~$28 billion annual cost[19] in the US alone. The number of adults with clot-related complications is estimated to reach ~1.82 million by 2050[20]. Blood clot formation through the coagulation cascade is a part of the natural response to injury and cut and prevents loss of blood from severed blood vessels[21]. The life-saving process of clot formation can become life-threatening if a blood vessel is blocked due to a clot. Indeed, pathologies of clot formation include heart attack, stroke, and pulmonary embolism account for ~50% of all hospital deaths. Reperfusion, the act of restoring blood flow, with tissue plasminogen activator (tPA) remains the gold standard treatment for ischemic stroke[22]. However, initiating tPA treatment after 3-4.5 hr of stroke onset can lead to adverse side effects, notably, hemorrhagic transformation (HT). Therefore, it is important to explore alternative approaches that could either replace tPA treatment or extend the time window for tPA perfusion beyond the current time frame[22]. The fibrinolytic system provides a mechanism of clot lysis and consists of plasminogen, which is converted to the active enzyme plasmin by tissue plasminogen activator (tPA) and urokinase plasminogen activator (uPA), which in turn degrades fibrin clot. The fibrinolytic system may be inhibited by specific plasminogen activator inhibitors (mainly PAI-1) or specific plasmin inhibitors (mainly α2-antiplasmin) or by thrombin-activatable fibrinolysis inhibitor (TAFI or procarboxypeptidase U).

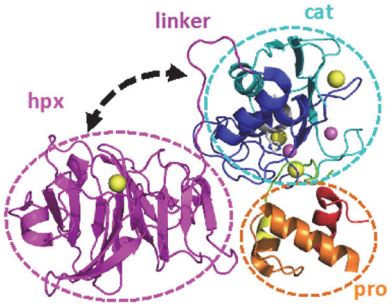

Figure 1. MMP1 structure. The hemopexin domain (hpx) is connected to the catalytic domain (cat) by a flexible linker that enables inter-domain dynamics and allosteric communication. The pro domain is cleaved off to activate MMPs for catalysis. Yellow and mauve spheres represent the van der Waals radii of the calcium and zinc atoms respectively.

While the usual fibrinolytic system consisting of tissue plasminogen activator (tPA) and plasminogen provides an effective mechanism of degradation of fibrinogen and crosslinked fibrin, the observation of fibrinolytic activity in plasminogen-deleted animals suggests alternative proteolytic pathways. Many proteases other than plasmin have been studied for fibrinolytic activity. For example, staphopain A (ScpA) and staphopain B (SspB), cysteine proteases released by pathogenic Gram-positive bacteria *Staphylococcus aureus*, impair clotting by degrading fibrinogen[23]. MMPs are potential alternatives in the fibrinolytic system because MMPs are found in pro[24,25] and activated[26-29] forms in blood. There are reports of fibrinolytic activity of MMP3[30], MMP9[31], and MT-MMP1[32], but the field is relatively unexplored[33]. Previously, MMP1 was reported to have insignificant fibrinolytic activity[30], which is in contrast to our observations.

Here we show that MMP1 inter-domain dynamics on fibrin are activity-dependent and can be modulated using ligands. At some functionally relevant MMP1 conformations, the two domains are far apart. These conformations appear more for active MMP1 in comparison to the inactive MMP1 and can be inhibited by tetracycline, an antibiotic that is known to inhibit MMP1 activity as well[34,35]. MMP1 degrades fibrin by cleaving the α-chain first, followed by β- and γ- chains. Interestingly, the catalytically inactive point mutant E219Q of MMP1 can still degrade the α- and β-chains even though the E219Q mutant is unable to cleave triple-helical type-1 collagen. Using molecular docking of MMP1 with a model of fibrin, we found that the proximity of MMP1 to the three fibrin chains are in excellent agreement with the experimentally observed sequence of degradation of the three chains.

Results and discussion

Single-molecule measurement of MMP1 inter-domain dynamics on fibrin. To measure MMP1 inter-domain dynamics, we measured single molecule FRET (smFRET) between two dyes attached to the catalytic and hemopexin domains of MMP1. To this end, we mutated S142 on the catalytic domain and S366 on the hemopexin domain of MMP1 to cysteines to attach dyes using maleimide chemistry. We selected a FRET pair, Alexa555 and Alexa647.

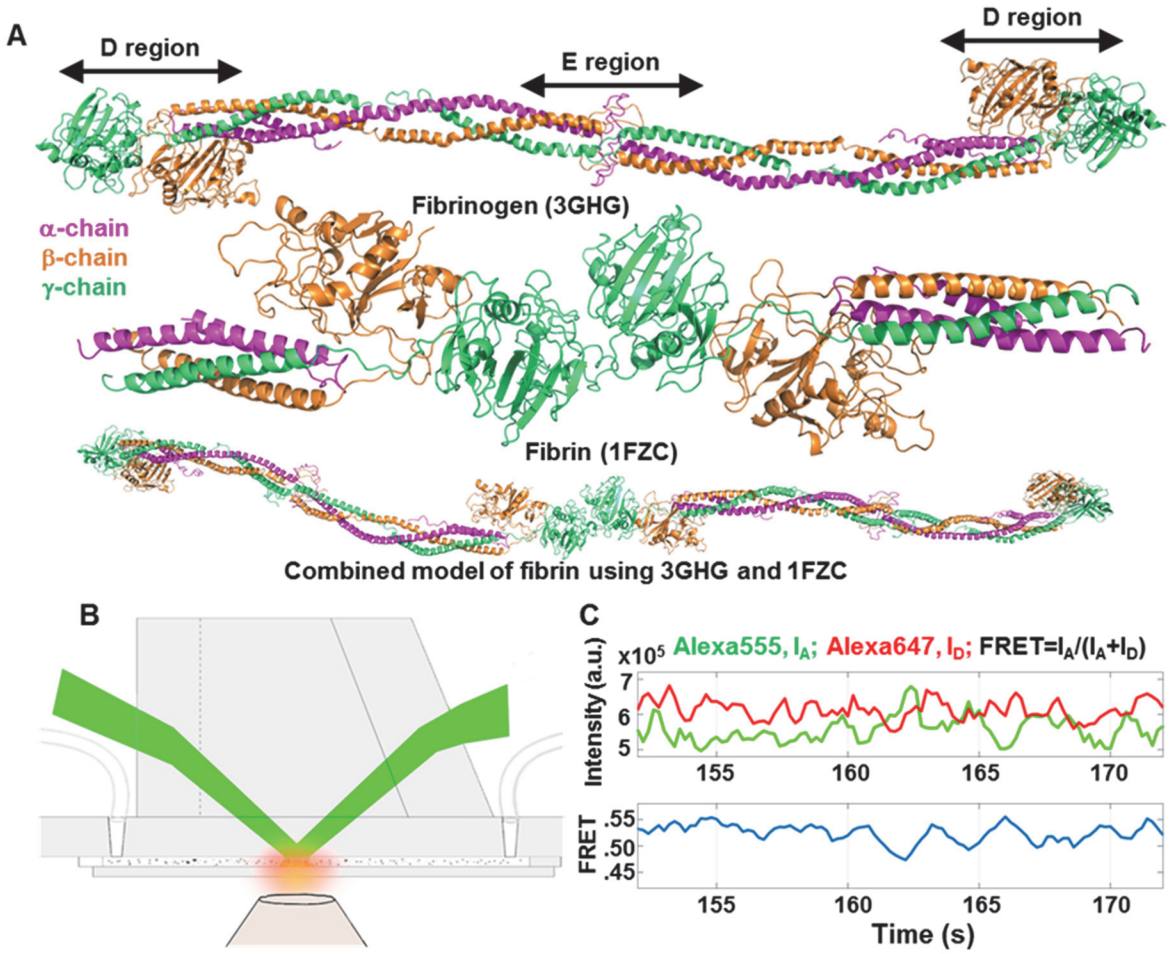

Figure 2. Single-molecule measurement of MMP1 dynamics on fibrin. (**A**) Crystal structure of fibrinogen (PDB ID: 3GHG) and fibrin (PDB ID: 1FZC). Water-soluble fibrinogen can polymerize into water-insoluble fibrin upon partial degradation by thrombin. (**B**) Schematics of the TIRF microscope. (**C**) Emission intensities of the two dyes. (top panel) Low FRET conformations lead to high Alexa555 emission, whereas High FRET conformations lead to Low Alexa555 emission. Anticorrelated Alexa647 and Alexa555 emissions, I_A and I_D respectively; (bottom panel) Calculated FRET trajectory to show MMP1 inter-domain dynamics.

We would detect smFRET only when both C142 and C366 are labeled with different dyes. There are also other potential complications. Photophysical properties of dyes depend on solution conditions (pH, temperature, chemical composition, etc.)[36], blinking due to transition into metastable states[37,38], and photobleaching due to reaction with oxygen in the excited state[39]. Additionally, Alexa dyes attached by a flexible linker[40] and enzyme microenvironment around dyes can change FRET[41]. The combined complexity of smFRET, solution conditions, and

128 simulations has been reported before[42]. To address the potential complications from labeling, we
129 compared the results for active (E219) and catalytically inactive point mutant (E219Q) MMP1.
130 Since active and inactive MMP1 will be affected equally by these complications, we can
131 distinguish the effects due to activity. Note that the amino acid E219[14] is the same as E200[4], which
132 differs because we included the 19 residues of signaling peptide as well. In a previous publication,
133 we showed that the specific activities of labeled and unlabeled MMP1 were not affected by
134 labeling. **Figure 2A** shows the structures of fibrinogen and fibrin as well as a reconstructed model
135 of fibrin using these structures. Upon limited cleavage by thrombin, water-soluble fibrinogen self-
136 assemble into water-insoluble fibrin. We measured MMP1 inter-domain dynamics on a thin layer
137 of water-insoluble fibrin in a flow cell using a Total Internal Reflection Fluorescence (TIRF)
138 microscope (**Figure 2B**) as described in our previous publications.

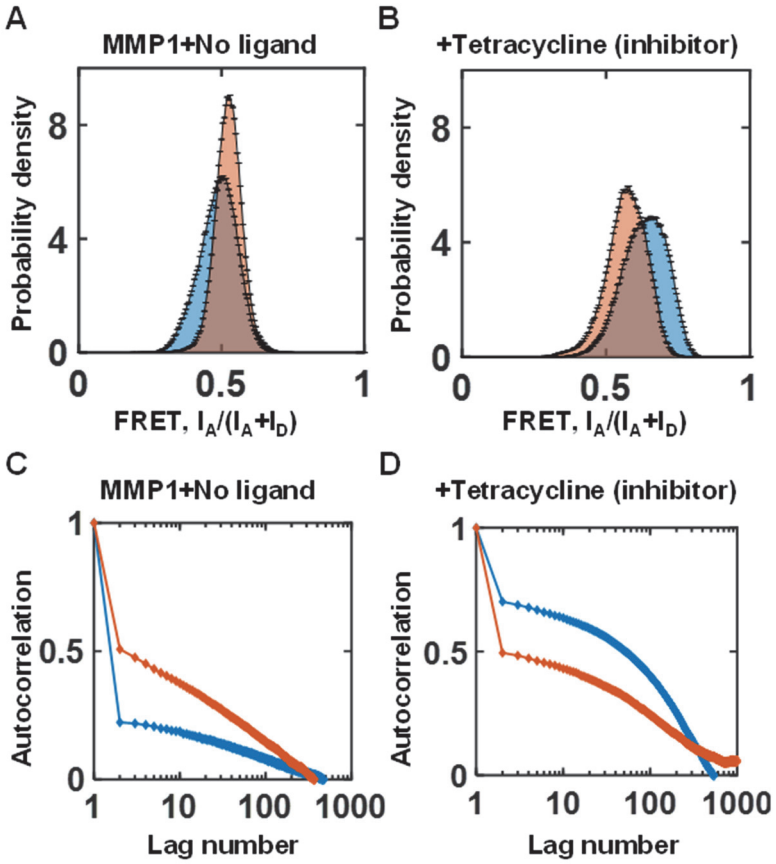

139 **Figure 3. Activity-dependent inter-domain dynamics of MMP1 on fibrin at 22ºC with 100 ms time**
140 **resolution.** Area-normalized histograms of MMP1 inter-domain distance for active (blue) and inactive
141 (orange) MMP1 (**A**) without ligand and (**B**) in the presence of tetracycline (an inhibitor). The error bars in
142 histograms represent the square roots of histogram bin counts. Autocorrelation of MMP1 inter-domain
143 distance for active (blue) and inactive (orange) MMP1 (**C**) without ligand and (**D**) in the presence of
144 tetracycline. The error bars in autocorrelations represent the standard error of the mean of autocorrelation
145 of individual FRET trajectories.

146 **MMP1 inter-domain dynamics on fibrin are correlated with activity and modulated by**
147 **ligands.** Each value of smFRET represents a conformation of MMP1. The histograms of smFRET
148 values measuring inter-domain distance (**Figure 3A**) for active and inactive MMP1 suggest that

low FRET conformations, where the two domains are far apart, occur more for active MMP1 (blue histogram) compared to inactive MMP1 (orange histogram). This observation suggests that the two domains need to move from each other for activity. Therefore, low FRET should appear more or less as MMP1 activity becomes more or less. To test, we used tetracycline that is known to affect MMP1 activity[35]. As shown in **Figure 3B**, low FRET conformations are significantly inhibited in the presence of tetracycline. Since correlated motions indicate a decrease in conformational entropy and can affect kinetics and thermodynamics of biological processes including catalysis[43], we calculated autocorrelation function of MMP1 conformational dynamics under different experimental conditions (**Figures 3C** and **3D**). Without any ligand, the correlation of FRET trajectories for active MMP1 was than the correlation for inactive MMP1 (**Figure 3C**). In the presence of tetracycline, this trend was reversed and inactive MMP1 had longer time-correlation than active MMP1 (**Figure 3D**). Taken together, these results strongly suggest that inter-domain dynamics and activity of MMP1 are functionally related and allosteric in nature. In addition, the presence of correlation in inter-domain dynamics means lower entropy (less randomness) and as such, the observed correlation suggests an entropy-driven activity

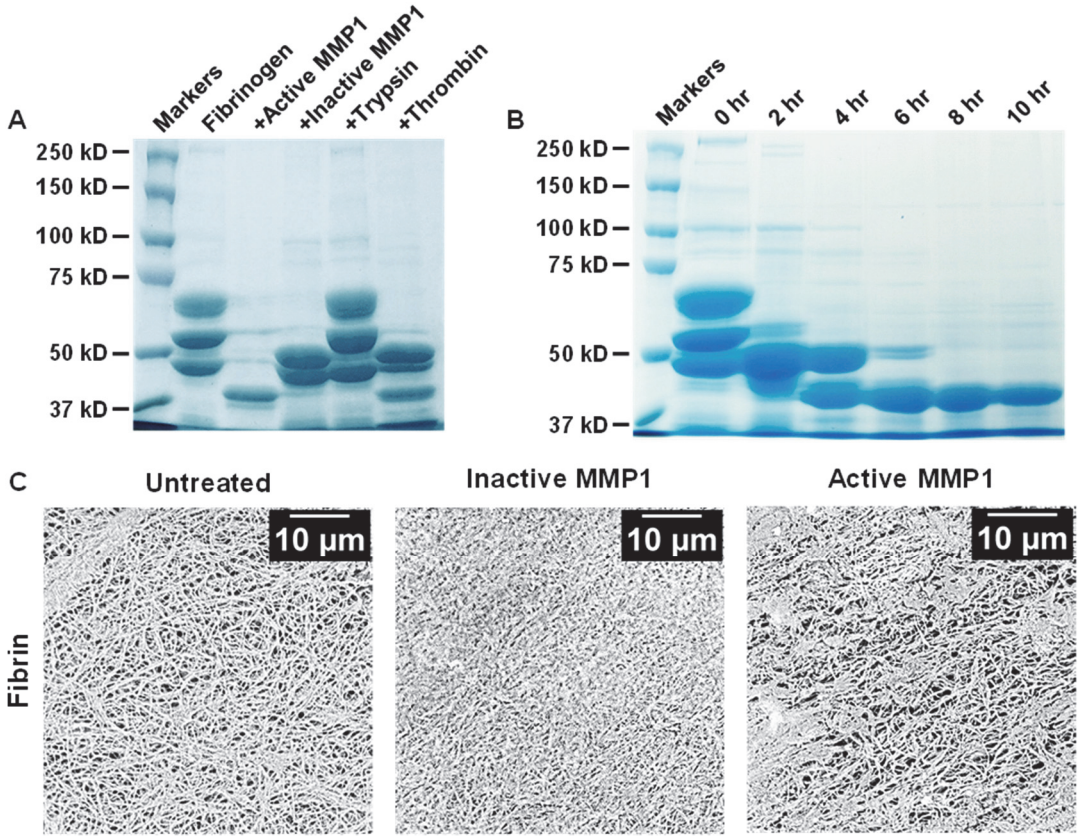

Figure 4. Ensemble activity of MMP1. (**A**) SDS PAGE of fibrinogen treated with different enzymes, but with trypsin inhibitor to eliminate the effect of trypsin using for MMP1 activation and purification. 1 mg/mL of fibrinogen was treated with 0.1 mg/mL enzymes and 0.5 mg/mL trypsin inhibitor. (**B**) Time-dependent fibrinogen degradation by active MMP1. (**C**) SEM image of fibrin with and without enzyme treatment.

Ensemble fibrinolytic activity of MMP1 shows changes in morphology and specific order of degradation of the three fibrin chains. Fibrinogen has three pairs of amino acid chains: 1) the α-chain with a molecular weight (MW) of ~63 kD, 2) the β-chain with MW of ~56 kD, and 3) the γ-chain with MW of ~47 kD. SDS PAGE of fibrinogen control approximately confirms MWs of

172 three chains (**Figure 4A**, lane 2 from left). These three chains are connected by a dimeric disulfide
173 knot (DSK) at the N-termini and at a second location along the length of fibrinogen. Treatment of
174 1 mg/mL of fibrinogen with 0.1 mg/mL of active MMP1 at 37° C for 24 hr resulted in cleavage of
175 all three chains and a final prominent fragment with MW of ~40 kD (**Figure 4A**, lane 3 from left).
176 The same experiment with catalytically inactive MMP1 with a point mutation E219Q at the
177 catalytic site degraded the α- and β- chains, but did not degrade the γ-chain (**Figure 4A**, lane 4
178 from left). We used trypsin during MMP1 purification and trypsin is known to degrade fibrinogen;
179 therefore, any residual trypsin could potentially interfere with the results. To address this
180 possibility, we added 0.5 mg/mL trypsin inhibitor to all the reactions, which was sufficient to
181 inhibit 0.1 mg/mL trypsin (**Figure 4A**, lane 5 from left). Even though limited digestion of
182 fibrinogen by thrombin leads to fibrin, the longer digestion for 24 hr led to further degradation of
183 fibrinogen and the profile looked in between active and inactive MMP1 (**Figure 4A**, lane 6 from
184 left). However, **Figure 4A** did not reveal the sequence in which the three chains of fibrinogen were
185 degraded. To determine the sequence, we incubated fibrinogen with active MMP1 for varying
186 amounts of time. MMP1 completely degraded α-chain and partially degraded β-chain within 2 hr;
187 however, γ-chain took almost more than 6 hr to be degraded (**Figure 4B**). After 8 hr, a primary
188 band at ~40 kD remained. Next, we tested the effects of MMP1 on fibrin morphology using SEM
189 (**Figure 4C**), where the destruction of fibrin structures was visible for active MMP1. Similar thin
190 layers of fibrin morphologies were created for smFRET experiments. Overall, ensemble
191 experiments in **Figure 4** showed that MMP1 has fibrinolytic activity on fibrinogen and fibrin, and
192 there was a specific sequence of degradation of the three chains. Both thrombin and trypsin cleave
193 the same Arg-Gly bonds in fibrinogen[44]. However, thrombin is highly specific and only four bonds
194 linking the fibrinopeptides to the rest of the fibrinogen molecule are rapidly hydrolyzed by
195 thrombin, whereas trypsin cleaves all peptide bonds in fibrinogen that follow arginine and lysine[44].
196 In comparison, degradation of fibrinogen and crosslinked fibrin by MMPs do not have specific
197 cleavage sites across the MMP-family. For example, MMP3, MMP7, and MT1-MMP cleave the
198 α-chain at Asp97-Phe98 and Asn102-Asn103; the β-chain at Asp123-Leu124, Asn137-Val138,
199 and Glu141-Tyr142; and the γ-chain at Thr83-Leu84[45]. Cleavage sites on both fibrinogen and
200 crosslinked fibrin for these three MMPs are in close proximity to those for plasmin. Additionally,
201 MMP3 solubilizes crosslinked fibrin by cleaving the Gly404-Ala405 bond in the γ-chain[30],
202 resulting in a D-like monomer fragment at ~94 kDa similar to fibrinogen degradation by plasmin.
203 In contrast, MMP7 and MT1-MMP solubilize crosslinked fibrin and produces D-like dimer
204 fragments at ~186 kDa similar to crosslinked fibrin degradation by plasmin[45]. However, MMP1,
205 MMP2, MMP9, and MT2-MMP do not show similar activity[45]. Fibrinogen degradation by
206 catalytic domains of MMP8, MMP12, MMP13, and MT1-MMP show differences in the cleavage
207 sites[46]. Overall, MMPs show differences in fibrinolytic activity, which is intriguing because the
208 catalytic domain is largely conserved among the MMP-family members[16]. Interestingly, MMP1
209 was reported to have little or no fibrinolytic activity[30], in stark contrast to our findings of significant
210 fibrinolytic activity of MMP1.

211 **The sequence of degradation correlates with the proximity of MMP1 to the three chains.** The
212 time-dependent degradation of fibrinogen (**Figure 4B**) showed that the overall catalytic activity is
213 fastest on the α-chain and slowest on the γ-chain. Since MMP1 needs to come in the proximity
214 before cleavage, we performed molecular docking of MMP1with fibrin. Since single molecule
215 experiments (**Figure 3**) informed that conformations with both longer and shorter inter-domain
216 distances are involved, we selected both open and close conformations of MMP1 (**Figure 5**). To
217 select the open conformation, we performed coarse-grained simulations of MMP1 (PDB ID 1SU3,

218 chain A) using Anisotropic Network Model (ANM) and selected the MMP1 conformation with
219 the highest inter-domain distance (**Figure 5A**, left panel). For close conformation, we selected the
220 conformation in the crystal structure (**Figure 5A**, right panel).

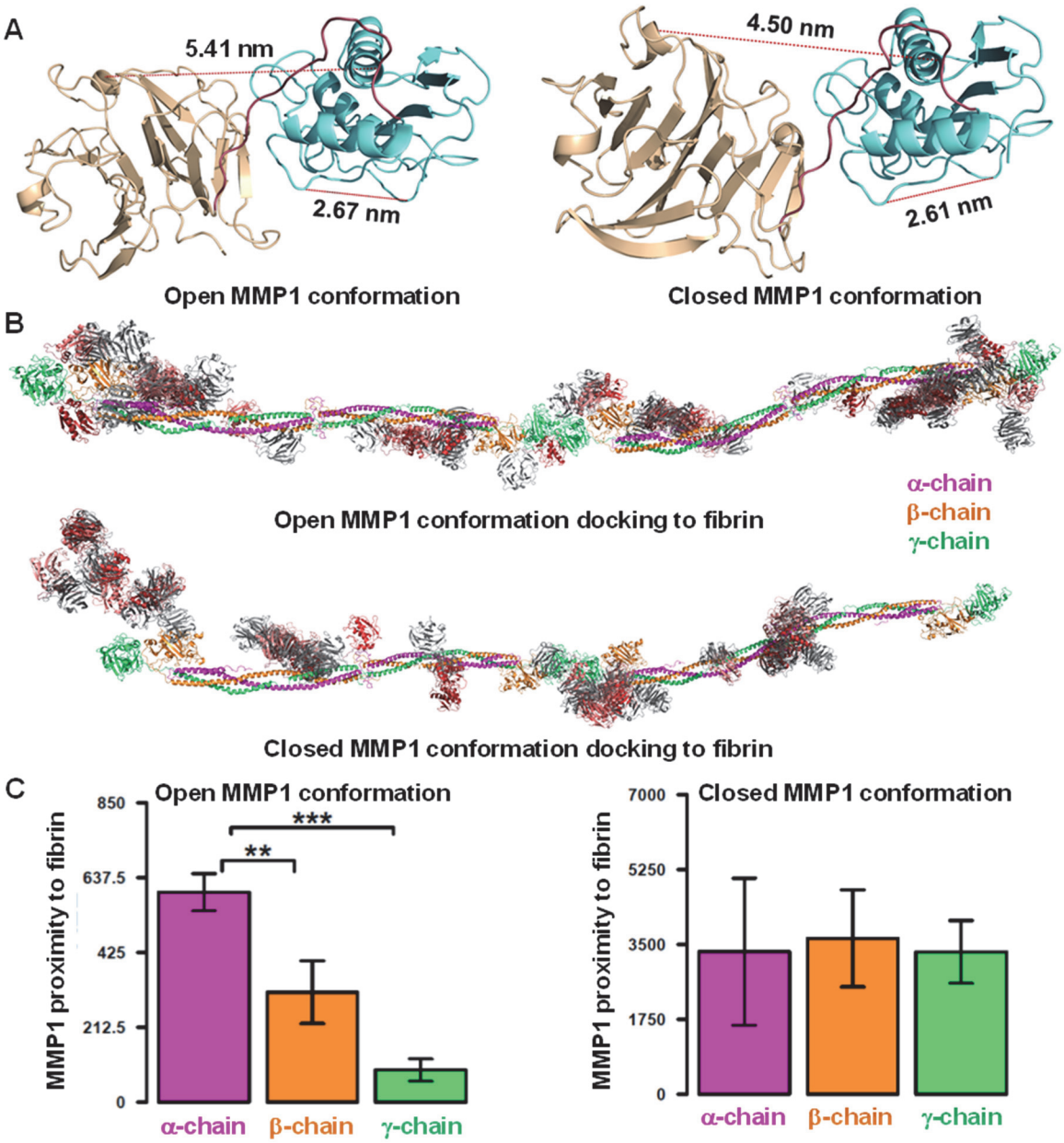

221 **Figure 5. Molecular docking of MMP1 with fibrin.** (**A**) Open MMP1 conformation as determined by the
222 inter-domain distance of conformations from ANM simulations; closed MMP1 conformation is determined
223 by the crystallographic conformation (PDB ID: 1SU3). (**B**) The clustered docking results obtained from
224 CLUSPRO using fibrin as the ligand and MMP1 as the receptor. The catalytic domain of MMP1 is red,
225 whereas the hemopexin domain is gray. (**C**) The distances between atoms in the three fibrin chains (set as
226 the ligands) and MMP1 (set as the receptor) were calculated from all docking poses obtained from
227 CLUSPRO. Any distance less than 5 Å was counted and the distributions of total count for each chain were
228 plotted for the open and closed conformations. p-value<0.05:*; p-value<0.01:**; p-value<0.001.

229 **Figure 5B** shows MMP1 molecular docking poses superimposed on the reconstructed model of
230 fibrin. MMP1 binds to fibrin at specific places in both open and close conformations; however,
231 both the catalytic and hemopexin domains of MMP1 bind at the same time more in the open
232 conformations. This is consistent with the single molecule observation that low FRET (open)
233 conformations are functionally relevant. To gain further insights, we calculated the distance
234 between every atom in the MMP1 and the three fibrin chains. We counted the number of distances
235 below 0.5 nm for the top 30 docking poses and calculated the mean and standard deviation (**Figure**
236 **5C**). On average, MMP1 in open conformation showed the closest proximity to the α-chain
237 (**Figure 5C**, left panel) and followed the experimentally observed sequence (**Figure 4B**). In
238 contrast, the close conformation of MMP1 did not show any significant difference in proximity to
239 the three chains (**Figure 5C**, right panel) validating further that open conformations observed in
240 the single molecule experiments are functionally relevant.

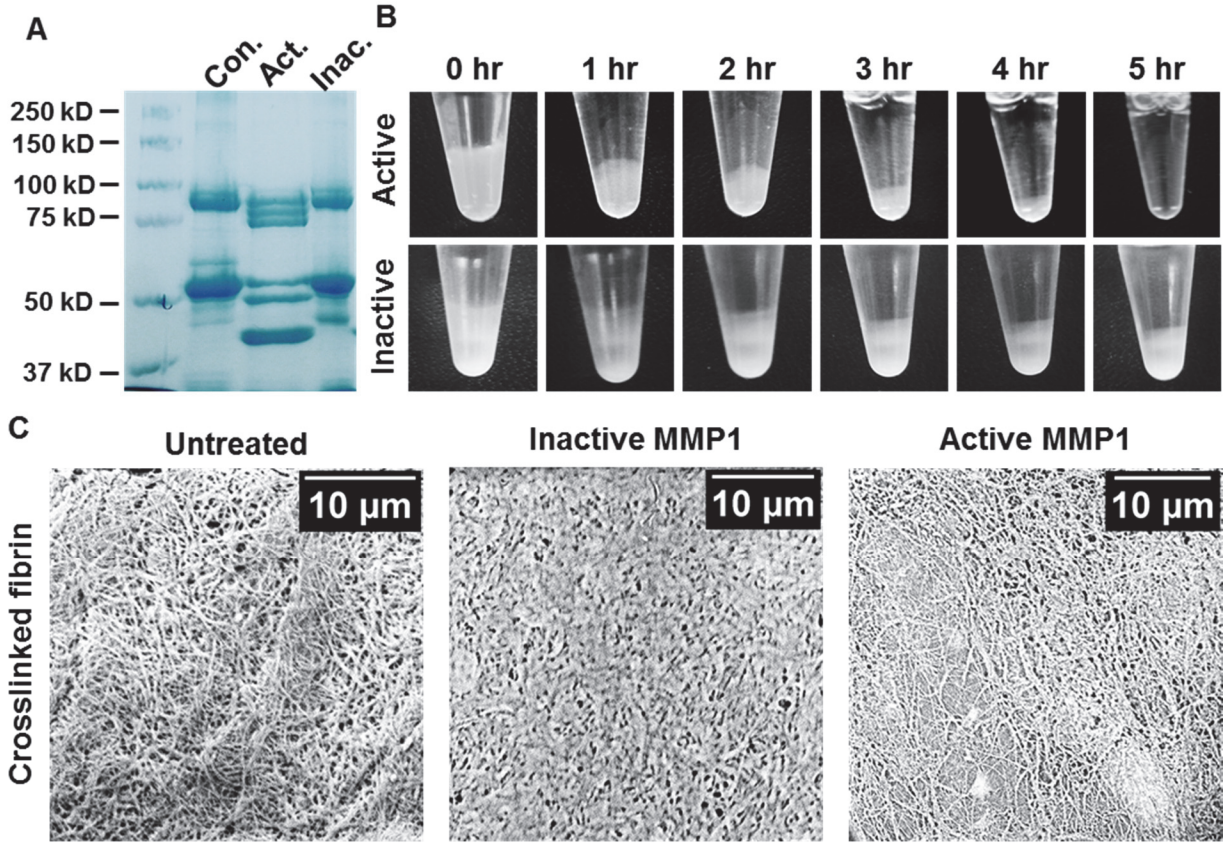

241

242 **Figure 6. Fibrinolytic activity of MMP1 on crosslinked fibrin.** (**A**) SDS PAGE of crosslinked fibrin
243 without (Conc.) and with active (Act.) and inactive MMP1 (Inac.). (**B**) 100 mg of wet crosslinked fibrin
244 treated with 0.1 mg/mL active and inactive MMP1 at 37ºC. (**C**) SEM image of crosslinked fibrin with and
245 without enzyme treatment. While thrombin alone can make fibrin, we need factor XIII and $CaCl_2$ in addition
246 to thrombin to make crosslinked fibrin.

247 **MMP1 efficiently degrades crosslinked fibrin.** It is known that water-soluble fibrinogen
248 becomes water-insoluble crosslinked fibrin in the presence of factor XIII, thrombin, and $CaCl_2$.
249 Thrombin converts fibrinogen to fibrin by cleaving both fibrinopeptide A and fibrinopeptide B and

250 exposing polymerization sites in the E region, which results in the soluble fibrin monomer[47]. Fibrin
251 monomers self-assemble into double-stranded protofibirls where the polymerization sites
252 noncovalently attach to the D regions of two other fibrin(ogen) molecules. Fibrin monomers in
253 each strand are arranged end to end, whereas monomers across the strands are arranged in a half-
254 staggered overlap. The γ-chains of adjacent D regions in each strand is covalently attached by
255 isopeptide bonds, which are formed due to the activity of factor XIIIa and appear as a ~94 kDa
256 band in SDS PAGE under reducing conditions (**Figure 6A**). Factor XIIIa can also catalyze
257 covalent isopeptide bonds between α-chains; however, these reactions are relatively slower. As a
258 result, the band at ~66.5 kDa due to the α-chains still appear in SDS PAGE (**Figure 6A**). Since
259 factor XIIIa does not crosslink the β-chains[48,49], the band at ~52 kDa due to the β-chains remains
260 unchanged in SDS PAGE of fibrinogen (**Figure 4A**) and crosslinked fibrin (**Figure 6A**). As shown
261 in **Figure 6B**, active MMP1 degrades and dissolves water-insoluble crosslinked fibrin, which is
262 inhibited by inactive MMP1. **Figure 6C** shows the surface morphology of crosslinked fibrin
263 imaged using SEM. Treatment with active MMP1 resulted in a more porous structure of
264 crosslinked fibrin.

265 In summary, we have shown that MMP1 has fibrinolytic activity on fibrinogen, fibrin, and
266 crosslinked fibrin. Single molecule measurements of MMP1 inter-domain dynamics on fibrin
267 revealed that activity is correlated with conformations where the catalytic and hemopexin domains
268 are far apart (open conformations) and led to low FRET in the single molecule measurements.
269 These open conformations are inhibited by a catalytically inactive point mutant E219Q of MMP1
270 and tetracycline, a well-known inhibitor of MMP1. Molecular docking showed that open
271 conformations bind to fibrin so that MMP1 was closest to the α-chain and farthest from the γ-chain
272 and as such, explained the experimental SDS PAGE profiles showing the sequence of degradation
273 of the three chains. Limited digestion of fibrin by MMP1 with and without crosslinks showed
274 increased porosity due to degradation. MMP1 degrades and dissolves crosslinked fibrin rapidly
275 suggesting an alternative to blood clot management.
276
277

Methods

Reconstruction of the extended fibrin molecule. To obtain the reconstructed model of fibrin, two independent instances of fibrinogen (PDB: 3GHG)[50] were superimposed to D-D fibrin fragment (PDB: 1FZC)[51] using the Combinatorial Extension (CE) algorithm[52] implemented in PyMOL[53]. The fibrinogen asymmetric unit presents two different biological assemblies (either the chains A-F+M-P or G-L+Q-T). Each of such biological assemblies has two ends, which are represented by chains A-C and chains D-F in the case of the first biological assembly and by chains G-I and J-L in the second biological assembly. Each of such fibrinogen ends could be superimposed to any of the ends of the fibrin crystal (either the chains A-C or chains D-F), yielding a total of 16 different possibilities to reconstruct the fibrin molecule. For each of the superimposed fibrinogen biological assembly, an additional instance of the fibrin crystal was superimposed to the fibrinogen biological assembly not used for the initial superimposition. Thus, two additional fibrin crystals (Fa and Fb, one per superimposed fibrinogen biological assembly) were superimposed on each of the 16 different reconstruction attempts. A reconstruction compatible with the original fibrinogen packing would show no differences in the positioning of Fa and Fb. Thus, to select the best superimposition combination to reconstruct the fibrin molecule, the one that minimized the RMSD in between Fa and Fb was selected.

Selection of close and open conformations of MMP1. The activation peptide (residues 32 to 98) was removed from the first biological assembly (chain A) of the crystal structure of MMP1 (PDB ID: 1SUA3), leaving only the catalytic (residue numbers 107 to 260), linker (261-277) and hemopexin (278-466) domains of the enzyme, which was selected as the close conformation. To obtain the open conformation, these coordinates were submitted to the ANM web server 2.1[54] using default parameters to obtain the three-dimensional fluctuation model coordinate files for the 20 slowest modes, requesting 20 frames per model. For each frame on each model, selected distances were calculated using PyMOL. Distances between S142 and S366 were used to analyze the fluctuations between the catalytic and homeopexin domains. The single frame that maximized this distance (second mode, second frame) was selected as the MMP1 open conformation.

Molecular docking of MMP1 with fibrin. The close and open conformations of MMP1 were docked with the reconstructed fibrin molecule using the ClusPro 2.0 webserver[55] and default parameters. The reconstructed fibrin was used as the receptor, whereas the MMP1 conformations were used as the ligands. The centroid structure of each of the resulting clusters (maximum 30) was considered as the representative docking solution for a cluster and the corresponding weighted scores for the best coefficient were obtained for each solution. All different solutions were brought to the same Cartesian space by aligning the reconstructed fibrin from each solution to a template one using PyMOL. To analyze the accessibility of MMP1 from each of the docking solutions to the different fibrin or fibrinogen chains, we counted the total number of times that any atom from MMP1 was within 5 Angstrom distance from any atom from each of the chains.

Preparation of fibrin without and with crosslinks. We prepared fibrin without crosslinks by adding 10 units of thrombin (Cayman chemical, Cat# 13188) to 50 µg of fibrinogen (Cayman chemical, Cat# 16088) and incubating at 37º C for 18 hr with 250 rpm shaking inside an incubator (Thermo Fisher Scientific, MaxQ600). Preparation of crosslinked fibrin involved two additional reagents: factor XIII (Abcam, Cat # ab62427) and $CaCl_2$. Formation of crosslinked fibrin involves

activation of human factor XIII to active human factor XIII_a and fibrinogen (pro form) to fibrin threads by thrombin, which in the presence of Ca^{++} induces crosslinking to form crosslinked fibrin. We added 10 units of thrombin to 2.5 µg of factor XIII in a 0.5 mL PCR tube, diluted with 10 mM Phosphate Buffer Saline (PBS) (Sigma, Cat# P3813, pH 7.4) to a total reaction volume of 100 µL, and incubated at 37º C for 10 min. After incubation, we added 50 µg of fibrinogen and 10 µL of 5 mM $CaCl_2$, diluted with PBS buffer to a total reaction volume of 200 µL, and incubated at 37º C for 15 min to obtain gel-like crosslinked fibrin. The surface morphology of fibrin was imaged using a Phenom Pro Scanning Electron microscope.

Single-molecule measurements. Full-length recombinant MMPs were expressed in *E. coli* and purified in activated form using a protease based purification method[14]. Purified MMP1 was labeled with AlexaFluor555 (ThermoFisher Scientific, Cat# A20346, donor dye) and AlexaFluor647 (ThermoFisher Scientific, Cat# A20347, acceptor dye) using maleimide chemistry. 1 mL of MMP1 at 1 mg/mL concentration was incubated with 20 µL of 1 mg/mL AlexaFluor555 and AlexaFluor647 for 1 hr in a 5 mL glass vial in a nitrogen environment to avoid oxidation of the dyes. After incubation, we used a 30 kDa cut-off Amicon filter to remove free dyes from the solution. We compared the specific activities of labeled and unlabeled MMP1 on the synthetic substrate, MCA-Lys-Pro-Leu-Gly-Leu-DPA-Ala-Arg-NH2, (R&D Systems, Cat# ES010) as described before[14]. A thin layer of fibrin was created on a quartz slide similar to blood smear protocol used in diagnostics[56]. Labeled MMP1 was excited at 532 nm inside a flow cell made from double-sided tape sandwiched between the quartz slide and a glass coverslip using the evanescent wave created at the interface of the quartz slide and sample in a Total Internal Reflection Fluorescence (TIRF) Microscope as described before[57,58]. Alexa647 and Alexa555 emissions were imaged by an EMCCD camera (Andor iXon). The two emission channels were superimposed using a pairwise stitching plugin of ImageJ and the intensities from the two dyes were extracted and analyzed using Matlab.

SDS PAGE. The degradation profile after fibrinolysis was analyzed using SDS-PAGE. We mixed SDS PAGE loading buffer containing BME (Biorad, Cat# 610737) with each sample in a 1:1 (v/v) ratio and incubated at 95º C for 10 min. The samples were loaded onto the wells of 8% Tris.glycine gels. Electrophoresis was run in Tris.glycine buffer (Biorad, Cat# 1610732) for 30 min at 50 V followed by 1 hr at 120V. The precision Plus protein kaleidoscope pre-stained protein standards (Biorad, Cat# 1610375) were used as molecular weight markers. The SDS-PAGE gel was stained with Coomassie Brilliant Blue R-250 (Biorad, Cat# 161-0436) and imaged after destaining.

ACKNOWLEDGMENTS

This project was partially funded by the professional development funds given to JKS and SKS at the Colorado School of Mines. JPI is supported by the grant MSCAfellow@MUNI.

AUTHOR CONTRIBUTIONS

L.K. and S.K.S. designed experiments, L.K. performed experiments, S.K. helped L.K. during experiments, J.P. performed docking and ANM analysis. L.K., J.P., J.K., C.H., J.K., and S.K.S. analyzed data. S.K.S. wrote the manuscript. All authors edited the manuscript.

COMPETING FINANCIAL INTERESTS

The authors declare no competing financial interests.

References

1 Rodríguez, D., Morrison, C. J. & Overall, C. M. Matrix metalloproteinases: what do they not do? New substrates and biological roles identified by murine models and proteomics. *Biochimica et Biophysica Acta (BBA)-Molecular Cell Research* **1803**, 39-54 (2010).

2 Page-McCaw, A., Ewald, A. J. & Werb, Z. Matrix metalloproteinases and the regulation of tissue remodelling. *Nature reviews. Molecular cell biology* **8**, 221-233, doi:10.1038/nrm2125 (2007).

3 Jackson, B. C., Nebert, D. W. & Vasiliou, V. Update of human and mouse matrix metalloproteinase families. *Human genomics* **4**, 194 (2010).

4 Manka, S. W. *et al.* Structural insights into triple-helical collagen cleavage by matrix metalloproteinase 1. *Proceedings of the National Academy of Sciences of the United States of America* **109**, 12461-12466, doi:10.1073/pnas.1204991109 (2012).

5 Karabencheva-Christova, T. G., Christov, C. Z. & Fields, G. B. Conformational Dynamics of Matrix Metalloproteinase-1· Triple-Helical Peptide Complexes. *The Journal of Physical Chemistry B* (2017).

6 Singh, W., Fields, G. B., Christov, C. Z. & Karabencheva-Christova, T. G. Importance of the linker region in matrix metalloproteinase-1 domain interactions. *RSC advances* **6**, 23223-23232 (2016).

7 Fields, G. B. Interstitial collagen catabolism. *J Biol Chem* **288**, 8785-8793, doi:10.1074/jbc.R113.451211 (2013).

8 Bertini, I. *et al.* Structural basis for matrix metalloproteinase 1-catalyzed collagenolysis. *Journal of the American Chemical Society* **134**, 2100-2110 (2012).

9 Chung, L. D. *et al.* Collagenase unwinds triple-helical collagen prior to peptide bond hydrolysis. *Embo Journal* **23**, 3020-3030 (2004).

10 Lauer-Fields, J. L., Juska, D. & Fields, G. B. Matrix metalloproteinases and collagen catabolism. *Biopolymers* **66**, 19-32 (2002).

11 Salsas-Escat, R., Nerenberg, P. S. & Stultz, C. M. Cleavage site specificity and conformational selection in type I collagen degradation. *Biochemistry* **49**, 4147-4158 (2010).

12 Nerenberg, P. S. & Stultz, C. M. Differential unfolding of alpha 1 and alpha 2 chains in type I collagen and collagenolysis. *Journal of Molecular Biology* **382**, 246-256 (2008).

13 Nerenberg, P. S., Salsas-Escat, R. & Stultz, C. M. Do collagenases unwind triple-helical collagen before peptide bond hydrolysis? Reinterpreting experimental observations with mathematical models. *Proteins: Structure, Function, and Bioinformatics* **70**, 1154-1161 (2008).

14 Kumar, L., Colomb, W., Czerski, J., Cox, C. R. & Sarkar, S. K. Efficient protease based purification of recombinant matrix metalloprotease-1 in E. coli. *Protein expression and purification* **148**, 59-67 (2018).

15 Eckhard, U. *et al.* Active site specificity profiling of the matrix metalloproteinase family: Proteomic identification of 4300 cleavage sites by nine MMPs explored with structural and synthetic peptide cleavage analyses. *Matrix Biology* **49**, 37-60 (2016).

16 Ratnikov, B. I. *et al.* Basis for substrate recognition and distinction by matrix metalloproteinases. *Proceedings of the National Academy of Sciences* **111**, E4148-E4155 (2014).

17 Piccard, H., Van den Steen, P. E. & Opdenakker, G. Hemopexin domains as multifunctional liganding modules in matrix metalloproteinases and other proteins. *Journal of leukocyte biology* **81**, 870-892 (2007).

18 Heit, J. A., Cohen, A. T. & Anderson, F. A. Estimated annual number of incident and recurrent, non-fatal and fatal venous thromboembolism (VTE) events in the US. (2005).

19 Mahan, C. E. *et al.* Venous thromboembolism: annualised United States models for total, hospital-acquired and preventable costs utilising long-term attack rates. *Thrombosis and haemostasis* **107**, 291-302 (2012).

20 Deitelzweig, S., Johnson, B., Lin, J. & Schulman, K. Prevalence of clinical venous thromboembolism in the USA: current trends and future projections. *American journal of hematology* **86**, 217-220 (2011).

21 Collen, D. The plasminogen (fibrinolytic) system. *Thrombosis and haemostasis* **82**, 259-270 (1999).

22 dela Peña, I., Borlongan, C., Shen, G. & Davis, W. Strategies to extend thrombolytic time window for ischemic stroke treatment: an unmet clinical need. *Journal of stroke* **19**, 50 (2017).

23 Ohbayashi, T. *et al.* Degradation of fibrinogen and collagen by staphopains, cysteine proteases released from Staphylococcus aureus. *Microbiology* **157**, 786-792 (2011).

24 Saito, S. *et al.* Role of matrix metalloproteinases 1, 2, and 9 and tissue inhibitor of matrix metalloproteinase-1 in chronic venous insufficiency. *Journal of Vascular Surgery* **34**, 930-937 (2001).

25 Asahi, M. *et al.* Role for matrix metalloproteinase 9 after focal cerebral ischemia, effects of gene knockout and enzyme inhibition with BB-94. *Journal of Cerebral Blood Flow and Metabolism* **20**, 1681-1689 (2000).

26 Fujimura, M. *et al.* Early appearance of activated matrix metalloproteinase-9 and blood-brain barrier disruption in mice after focal cerebral ischemia and reperfusion. *Brain Research* **842**, 92-100 (1999).

27 Koshiba, T. *et al.* Detection of matrix metalloproteinase activity in human pancreatic cancer. *Surgery Today-the Japanese Journal of Surgery* **27**, 302-304 (1997).

28 Hanemaaijer, R., Visser, H., Konttinen, Y. T., Koolwijk, P. & Verheijen, J. H. A novel and simple immunocapture assay for determination of gelatinase-B (MMP-9) activities in biological fluids: Saliva from patients with Sjogren's syndrome contain increased latent and active gelatinase-B levels. *Matrix Biology* **17**, 657-665 (1998).

29 Sakalihasan, N., Delvenne, P., Nusgens, B. V., Limet, R. & Lapiere, C. M. Activated forms of MMP(2) and MMP(9) in abdominal aortic aneurysms. *Journal of Vascular Surgery* **24**, 127-133 (1996).

30 Bini, A., Itoh, Y., Kudryk, B. J. & Nagase, H. Degradation of Cross-Linked Fibrin by Matrix Metalloproteinase 3 (Stromelysin 1): Hydrolysis of the γ Gly 404− Ala 405 Peptide Bond. *Biochemistry* **35**, 13056-13063 (1996).

31 Lelongt, B. *et al.* Matrix Metalloproteinase 9 Protects Mice from Anti–Glomerular Basement Membrane Nephritis through Its Fibrinolytic Activity. *Journal of Experimental Medicine* **193**, 793-802 (2001).

32 Hotary, K. B. *et al.* Matrix metalloproteinases (MMPs) regulate fibrin-invasive activity via MT1-MMP–dependent and–independent processes. *Journal of Experimental Medicine* **195**, 295-308 (2002).

460 33 Lijnen, H. Matrix metalloproteinases and cellular fibrinolytic activity. *Biochemistry*
461 *(Moscow)* **67**, 92-98 (2002).
462 34 Acharya, M. R., Venitz, J., Figg, W. D. & Sparreboom, A. Chemically modified
463 tetracyclines as inhibitors of matrix metalloproteinases. *Drug Resistance Updates* **7**, 195-
464 208 (2004).
465 35 Golub, L. *et al.* Tetracyclines inhibit tissue collagenase activity. *Journal of periodontal*
466 *research* **19**, 651-655 (1984).
467 36 Stennett, E. M., Ciuba, M. A. & Levitus, M. Photophysical processes in single molecule
468 organic fluorescent probes. *Chemical Society Reviews* **43**, 1057-1075 (2014).
469 37 Cordes, T., Vogelsang, J. & Tinnefeld, P. On the mechanism of Trolox as antiblinking and
470 antibleaching reagent. *Journal of the American Chemical Society* **131**, 5018-5019 (2009).
471 38 Rasnik, I., McKinney, S. A. & Ha, T. Nonblinking and long-lasting single-molecule
472 fluorescence imaging. *Nature methods* **3**, 891 (2006).
473 39 Kochevar, I. E. & Redmond, R. W. in *Methods in enzymology* Vol. 319 20-28 (Elsevier,
474 2000).
475 40 Best, R. B. *et al.* Effect of flexibility and cis residues in single-molecule FRET studies of
476 polyproline. *Proceedings of the National Academy of Sciences* **104**, 18964-18969 (2007).
477 41 Levitus, M. & Ranjit, S. Cyanine dyes in biophysical research: the photophysics of
478 polymethine fluorescent dyes in biomolecular environments. *Quarterly reviews of*
479 *biophysics* **44**, 123-151 (2011).
480 42 Merchant, K. A., Best, R. B., Louis, J. M., Gopich, I. V. & Eaton, W. A. Characterizing
481 the unfolded states of proteins using single-molecule FRET spectroscopy and molecular
482 simulations. *Proceedings of the National Academy of Sciences* **104**, 1528-1533 (2007).
483 43 Jarymowycz, V. A. & Stone, M. J. Fast time scale dynamics of protein backbones: NMR
484 relaxation methods, applications, and functional consequences. *Chemical reviews* **106**,
485 1624-1671 (2006).
486 44 Andreatta, R. H., Liem, R. K. & Scheraga, H. A. Mechanism of action of thrombin on
487 fibrinogen, I. Synthesis of fibrinogen-like peptides, and their proteolysis by thrombin and
488 trypsin. *Proceedings of the National Academy of Sciences* **68**, 253-256 (1971).
489 45 Bini, A., Wu, D., Schnuer, J. & Kudryk, B. J. Characterization of stromelysin 1 (MMP-3),
490 matrilysin (MMP-7), and membrane type 1 matrix metalloproteinase (MT1-MMP) derived
491 fibrin (ogen) fragments D-dimer and D-like monomer: NH2-terminal sequences of late-
492 stage digest fragments. *Biochemistry* **38**, 13928-13936 (1999).
493 46 Hiller, O., Lichte, A., Oberpichler, A., Kocourek, A. & Tschesche, H. Matrix
494 metalloproteinases collagenase-2, macrophage elastase, collagenase-3, and membrane type
495 1-matrix metalloproteinase impair clotting by degradation of fibrinogen and factor XII.
496 *Journal of Biological Chemistry* **275**, 33008-33013 (2000).
497 47 Medved, L., Weisel, J., FIBRINOGEN, THROMBOSIS, F. X. S. O. T. S. S. C. O. T. I. S.
498 O. & HAEMOSTASIS. Recommendations for nomenclature on fibrinogen and fibrin.
499 *Journal of Thrombosis and Haemostasis* **7**, 355-359 (2009).
500 48 McKee, P. A., Mattock, P. & Hill, R. L. Subunit structure of human fibrinogen, soluble
501 fibrin, and cross-linked insoluble fibrin. *Proceedings of the National Academy of Sciences*
502 **66**, 738-744 (1970).
503 49 Sobel, J. H. & Gawinowicz, M. A. Identification of the α chain lysine donor sites involved
504 in factor XIIIa fibrin cross-linking. *Journal of Biological Chemistry* **271**, 19288-19297
505 (1996).

50 Kollman, J. M., Pandi, L., Sawaya, M. R., Riley, M. & Doolittle, R. F. Crystal structure of human fibrinogen. *Biochemistry* **48**, 3877-3886 (2009).

51 Everse, S. J., Spraggon, G., Veerapandian, L., Riley, M. & Doolittle, R. F. Crystal structure of fragment double-D from human fibrin with two different bound ligands. *Biochemistry* **37**, 8637-8642 (1998).

52 Shindyalov, I. N. & Bourne, P. E. Protein structure alignment by incremental combinatorial extension (CE) of the optimal path. *Protein engineering* **11**, 739-747 (1998).

53 Schrodinger, L. The PyMOL molecular graphics system, version 1.8. *Schrodinger LLC, New York, NY* (2015).

54 Eyal, E., Lum, G. & Bahar, I. The anisotropic network model web server at 2015 (ANM 2.0). *Bioinformatics* **31**, 1487-1489 (2015).

55 Kozakov, D. *et al.* The ClusPro web server for protein–protein docking. *Nature protocols* **12**, 255 (2017).

56 Bain, B. J. Diagnosis from the blood smear. *New England Journal of Medicine* **353**, 498-507 (2005).

57 Dittmore, A. *et al.* Internal strain drives spontaneous periodic buckling in collagen and regulates remodeling. *Proceedings of the National Academy of Sciences*, 201523228 (2016).

58 Sarkar, S. K., Marmer, B., Goldberg, G. & Neuman, K. C. Single-molecule tracking of collagenase on native type I collagen fibrils reveals degradation mechanism. *Current biology : CB* **22**, 1047-1056, doi:10.1016/j.cub.2012.04.012 (2012).